AAPS PharmSciTech **2004; 5 (1) Article 10 (http://www.aapspharmscitech.org).**

Effect of Vacuum Drying on Protein-Mannitol Interactions: The Physical State of Mannitol and Protein Structure in the Dried State

Submitted: October 20, 2003; Accepted: January 9, 2004

Vikas K. Sharma[1,2] and Devendra S. Kalonia[1]

[1]Department of Pharmaceutical Sciences, University of Connecticut, Storrs, CT 06269
[2]Present address: Biotechnology Process Engineering Center, and Department of Chemistry, Massachusetts Institute of Technology, Cambridge, MA 02139

ABSTRACT

The purpose of the present studies was to systematically investigate protein-mannitol interactions using vacuum drying, to obtain a better understanding of the effect of protein/mannitol wt/wt ratios on the physical state of mannitol and protein secondary structure in the dried state. Solutions containing β-lactoglobulin (βLg):mannitol (1:1-1:15 wt/wt) were vacuum dried at 5°C under 3000 mTorr of pressure. The physical state of mannitol was studied using x-ray powder diffractometry (XRPD), polarized light microscopy (PLM), Fourier-transform infrared (FTIR) spectroscopy, and modulated differential scanning calorimetry (MDSC). XRPD studies indicated that mannitol remained amorphous up to 1:5 wt/wt βLg:mannitol ratio, whereas PLM showed the presence of crystals of mannitol in all dried samples except for the 1:1 wt/wt βLg:mannitol dried sample. FTIR studies indicated that a small proportion of crystalline mannitol was present along with the amorphous mannitol in dried samples at lower (less than 1:5 wt/wt) βLg:mannitol ratios. The T_g of the dried 1:1 wt/wt βLg:mannitol sample was observed at 33.4°C in MDSC studies, which indicated that at least a part of mannitol co-existed with protein in a single amorphous phase. Evaluation of the crystallization exotherms indicated that irrespective of the βLg:protein wt/wt ratio in the initial sample, the protein to amorphous mannitol ratio was below 1:1 wt/wt in all dried samples. Second-derivative FTIR studies on dried βLg and recombinant human interferon α-2a samples showed that mannitol affected protein secondary structure to a varying degree depending on the overall mannitol content in the dried sample and the type of protein.

KEYWORDS: mannitol, proteins, vacuum drying, amorphous, protein structure

Corresponding Author: Devendra S. Kalonia, U-2092, School of Pharmacy, University of Connecticut, Storrs, CT 06269; Tel: (860) 486-3655; Fax: (860) 486-4998; Email: kalonia@uconn.edu

INTRODUCTION

Recently, there has been an increased level of interest in developing drying technologies in addition to lyophilization to formulate proteins as dry powders. The need has been generated to overcome some of the issues associated with the process of lyophilization that include long processing times (typically 3-5 days), expensive set up and maintenance of the lyophilization plants, and, most of all, the instabilities incurred upon proteins because of the inherent steps involved during freeze-drying.[1,2] The alternative technologies to lyophilization that have been developed recently include spray-drying,[3,4] spray-freeze drying,[5] bulk crystallization,[6] supercritical fluid technology,[7,8] vacuum drying,[9] and foam drying.[10] Due to the complex structural properties, proteins have a tendency to denature and undergo irreversible aggregation during various processing steps of drying.[11-13] The general strategy to stabilize proteins against drying and dehydration stresses is to use sugars such as trehalose or sucrose. The protective action of these sugars is attributed to their water-substituent properties,[14-16] which would preserve protein native structure upon loss of water, and/or their tendency to form stable glassy matrices,[17-19] which would provide a kinetic barrier for protein denaturation or aggregation to occur.

Mannitol is often added in dried protein formulations as the bulking agent as it has the tendency to crystallize rapidly from aqueous solutions. However, the physical state of mannitol depends on the processing steps, and improper control of the drying process can significantly affect the physical properties of mannitol in terms of its crystallization behavior. For example, manipulation of the freezing cycle can result in the formation of either amorphous mannitol or crystalline mannitol depending on the duration and the cooling rate during the freezing step of lyophilization.[20,21] Studies have been reported on the effect of mannitol on the stability of proteins during freeze-drying,[22,23] spray-drying,[24] and microsphere preparation.[25] It has been shown that, in general, protein stability depended on the physical state of mannitol, and crystalline mannitol was ineffective in preserving protein activity. Investigations have shown that

mannitol crystallinity is affected by the presence of a cosolute such as proteins, buffer components, or sugars.[20,21] Although these investigations indicated that a certain cosolute to mannitol ratio is required for the mannitol to remain amorphous, there has been no detailed systematic study to investigate the effect of the protein:mannitol ratio on the crystallinity of mannitol. In certain instances, for example, a higher protein:mannitol ratio (1:50 wt/wt) has been used to investigate protein-mannitol interactions,[23] whereas, in other studies, it has been reported that mannitol crystallinity is inhibited even at a much lower protein:mannitol wt/wt ratio.[24] It is also important to note that in almost all of the studies performed to investigate protein-mannitol interactions, freeze-drying or spray-drying has been used as the drying process. These processes by themselves have the tendency to affect protein structure and stability because of the inherent steps involved such as freezing, presence of ice/water interface (in case of freeze-drying,) or generation of a large air/water interface (in case of spray-drying). Hence, it would be difficult to ascertain whether an alteration in protein stability or structure in the presence of mannitol is due to the effect of the process or the inability of the excipient (ie, mannitol) to preserve protein structure/stability.

Therefore, the goal of the present studies was to systematically investigate protein-mannitol interactions using a simple drying process (ie, vacuum drying) in order to obtain a better understanding of the physical state of mannitol in the presence of proteins and its effect on the secondary structure of proteins. Vacuum drying was used in these studies because it offered a simple means of removal of water without any additional complications encountered in other processes. A multitude of techniques such as x-ray powder diffraction (XRPD), polarized light microscopy (PLM), modulated differential scanning calorimetry (MDSC), and Fourier-transform infrared spectroscopy (FTIR) were used for a comprehensive analysis. The emphasis has been placed on studying the effect of varying protein:mannitol wt/wt ratios on the physical state of mannitol using beta-lactoglobulin (βLg) as a model protein and on quantification of the amorphous and crystalline contents of mannitol in the dried samples.

Mannitol is a nonreducing acyclic sugar commonly used in pharmaceutical formulations. Mannitol is known to exist primarily in 3 main polymorphic forms designated as α, β, and δ forms that can be prepared by altering solution conditions and drying rates. Recently a monohydrate form of mannitol that is formed during freeze-drying has also been reported.[26] The spectral features of these polymorphs have been discussed elsewhere.[27,28] The commercially available mannitol mainly comes as the β-polymorph, which is also the thermodynamically stable form of mannitol at room temperature.

βLg was used as the model protein for the characterization of physical state of mannitol because of its ease of commercial availability in large quantities in the lyophilized form. To study the effect of mannitol on the secondary structure of proteins, studies were performed using βLg and recombinant interferon α-2a (IFNα2a). The 2 proteins were chosen for secondary structure analysis because of the differences in their secondary structure content (βLg predominantly has beta sheets, whereas IFNα2a is an all alphα-helical protein). βLg is an 18-kDa protein that exists as a dimer at pH 7.4. The isoelectric point (pI) of βLg is about 5.0, hence it possesses a net negative charge at pH 7.4. IFNα2a is a monomeric (from size exclusion chromatography-light scattering and velocity sedimentation studies; data not shown), 19-kDa protein, and the pI of this protein is in the range of 6.0 to 7.0. Hence, at pH 5.0 (pH of the solution at which IFNα2a was supplied), IFNα2a has a net positive charge.

MATERIALS AND METHODS

Materials

All buffer reagents and chemicals used in the present studies were of highest purity grade available from commercial sources and were used without further purification. D-mannitol was obtained as a fine crystalline powder *United States Pharmacopeia* grade from Cerestar USA Inc (Hammond, IN). Beta-lactoglobulin was obtained from Sigma-Aldrich (product no. L-3908, St Louis, MO) as a lyophilized powder (lyophilized from deionized water). Interferon α-2a (IFNα2a) was donated generously by Hoffman-La Roche (Nutley, NJ) and was supplied as a 1.6-mg/mL solution in pH 5.0 acetate buffer. Double distilled water, filtered through a 0.22-μm Millipore Millex filter (Millipore Corp, Billerica, MA) was used for preparation of all solutions.

Vacuum Drying

Dried samples of protein and mannitol were prepared by vacuum drying aqueous solutions containing βLg and mannitol in 1:1, 1:2, 1:5, 1:10, and 1:15 wt/wt ratios. Using a molecular weight of 36 000 Da for βLg dimer, these wt/wt ratios correspond to 1:198, 1:396, 1:989, 1:1980, and 1:2967 molar ratios of βLg:mannitol, respectively. The solutions were prepared in 10 mM phosphate buffer, pH 7.4, with ionic strength adjusted to 100 mM using sodium chloride. In brief, lyophilized βLg was dissolved in buffer and then added to mannitol solutions of varying concentrations to achieve desired βLg:mannitol ratio. For drying, 1 mL of each solution (in triplicate) was placed in 10-mL glass vials (West Pharmaceutical Co, Lionville, PA), and drying was performed using an FTS Dura-stop freeze-dryer (FTS sys-

tems Inc, Stoneridge, NY) at an initial controlled shelf temperature of 25°C under 3000 mTorr of pressure. During drying, the product temperature dropped down to ~0°C within 5 to 10 minutes. As the product temperature started increasing and reached close to 5°C, the shelf temperature was also reduced to 5°C, and the drying was then performed at a shelf temperature of 5°C for 24 hours. The vials were finally stoppered under vacuum and stored at -20°C for further analysis. The final product appeared as a highly porous dried mass inside the vial.

Moisture Analysis

Moisture analysis was performed on dried samples using an Orion AF7LC Coulometric Karl Fischer Titrimeter (Orion Research Inc., Boston, MA). The samples were suspended/dissolved in anhydrous methanol, and the moisture content was determined using anhydrous methanol as blank. All vacuum-dried samples had a final moisture content in the range of 0.5% to 1.2% wt/wt irrespective of the physical state or content of the protein or mannitol at the end of the 24-hour vacuum-drying period. All samples were stored in sealed vials (sealed within the dryer at the end of drying), and physical characterization was performed within 24 to 48 hours. No change in the moisture content was observed at the end of this storage time.

X-Ray Powder Diffraction

XRPD scans of dried samples were obtained on a Brucker D5005 x-ray diffractometer (Brucker AXS Inc, Madison, WI) using a CuKα radiation of wavelength 0.154 nm (voltage 40 kV, current 40 mA) from 2° to 40° range of 2θ at a scan rate of 0.5°/min. Approximately 100 mg of the dried product was placed on the flat polymer-based sample holder. All scans were normalized with respect to the counts per second to remove the variability in the intensity caused by slightly different powder amounts. The XRPD patterns obtained for mannitol in all samples were compared with the standard scans for identification of the mannitol polymorphs.[27,28] The abscissa of the scans is presented in 2θ angles and can be converted to d-spacings (in Angstroms, to remove wavelength dependence of peaks) using Bragg's equation (ie, $\lambda = 2d\sin\theta$, where λ is the wavelength of the radiation).

Polarized Light Microscopy

Vacuum-dried samples were analyzed for crystallinity using PLM (Micro-Tech Optical (NE) Inc, Bloomfield, CT). A few milligrams of the samples were placed on a glass slide under a drop of immersion liquid and covered with a coverslip. Dried samples were viewed under magnification ×40, and the pictures were captured and stored using a Sony Hyper HAD color video camera (Sony, New York, NY).

Fourier-Transform Infrared Spectroscopy (Mannitol Characterization)

FTIR spectroscopy was used to characterize the amorphous and crystalline polymorphs of mannitol. FTIR scans of dried samples containing mannitol were collected on a Nicolet Magma 560 FTIR spectrometer equipped with a dTGS detector. For each dried sample, an amount equivalent to approximately 1.0 mg of mannitol was mixed with 150 mg of dried KBr to produce the KBr pellet. A total of 100 scans were accumulated at 4-cm^{-1} instrument resolution in the region of 4000 cm^{-1} to 400 cm^{-1}.

Modulated Differential Scanning Calorimetry

MDSC scans on dried samples were obtained on a TA Instruments 2920 Modulated DSC equipped with a refrigerated cooling system and calibrated using indium (TA Instruments Inc, New Castle, DE). The dried samples were hermetically sealed in aluminum pans in dry nitrogen environment. All scans were obtained in the range of -20°C to 200°C at a scan rate of 2°C/min with a modulation of 0.5°C/min. The scans were normalized for the weight of mannitol in the sample that was placed in the pan and analyzed using Universal Analysis software provided by TA Instruments.

For quantification of the amorphous mannitol in the dried state, a known amount of the dried sample (in triplicate) for various wt/wt ratios was placed in the DSC pan. The area under the crystallization exotherm was calculated using the Universal Analysis software and normalized for the weight of mannitol. Since all of the mannitol was present in the amorphous state in the 1:1 βLg:mannitol wt/wt ratio (from XRPD and PLM results), the heat of crystallization from this sample was used to calculate the amount of amorphous mannitol in other samples. The methodology is discussed in more detail in the MDSC results section.

Fourier-Transform Infrared Spectroscopy (Protein Secondary Structure)

The secondary structure of rhIFN and βLg in vacuum-dried samples was evaluated by obtaining area-normalized second derivative FTIR spectra using a Nicolet Magna 560 FTIR spectrometer equipped with a dTGS detector. The spectra of dried protein powders were collected in the transmission mode using KBr pellets prepared by mixing samples containing equivalent of 0.5 to 1 mg protein in 150 mg of dried

Table 1. Specific XRPD Peak Positions Characteristic of Various Polymorphs of Mannitol Used for Polymorph Identification Along With Their Reported Melting Points*

	α Polymorph	β Polymorph	δ Polymorph
Distinguishing XRPD peak positions†	13.6° 17.2°	10.4° 14.6° 23.4°	9.7° 22.2°
Melting points‡	166°C	166.5°C	150°C-158°C

*XRPD indicates x-ray powder diffractometry.
†Data from Burger et al.[27]
‡Data from Yu et al.[26]

KBr under dry nitrogen environment. The pellet preparation was performed using a previously described procedure that was modified slightly.[29,30] Instead of placing the whole die in vacuum overnight, only KBr was dried overnight. The protein-KBr mixtures were prepared under dry nitrogen environment, and the pellets were pressed in vacuum under 12 tons of hydraulic pressure. A total of 100 scans were accumulated in the 4000 to 400 cm^{-1} region at 4-cm^{-1} instrument resolution. The original scans were smoothed using an 11-point smoothing function, and the second derivatives of these scans were obtained in the 1750 to 1550 cm^{-1} region (amide I). The second derivative spectra were baseline subtracted and finally area-normalized to unit area for relative comparisons.

RESULTS AND DISCUSSION

Characterization of Physical State of Mannitol in Vacuum-Dried Protein-Mannitol Samples

XRPD Studies

The 3 main polymorphs of mannitol (ie, α, β, and δ forms) exhibit distinct 2θ peaks in XRPD scans that can be used to identify the type of polymorph present in a given sample.[27,28] Some characteristic peaks of these 3 forms along with their reported melting points are shown in Table 1. The peak positions listed for each mannitol polymorph are those, which are not present in the other 2 polymorphs, hence the absence or presence of these listed peaks in the XRPD scan would clearly indicate the type of polymorphs present in the dried sample.

Figure 1 shows the XRPD scans of pure mannitol and of mannitol dried from water and buffer. The XRPD pattern of commercial mannitol used in these studies showed sharp peaks at 23.4°, 14.6°, and 10.4° 2θ that were characteristic of the crystalline β-polymorph (Table 1). This finding was also confirmed by the presence of a melting point peak ~166°C (DSC studies not shown). When dried from water or buffer, additional peaks were observed at 22.2° and 25.3° 2θ in the XRPD scans, indicating the presence of δ-polymorph along with β-polymorph. The presence of α-polymorph was ruled out because no peaks were observed at either 13.6° or 17.2° 2θ.

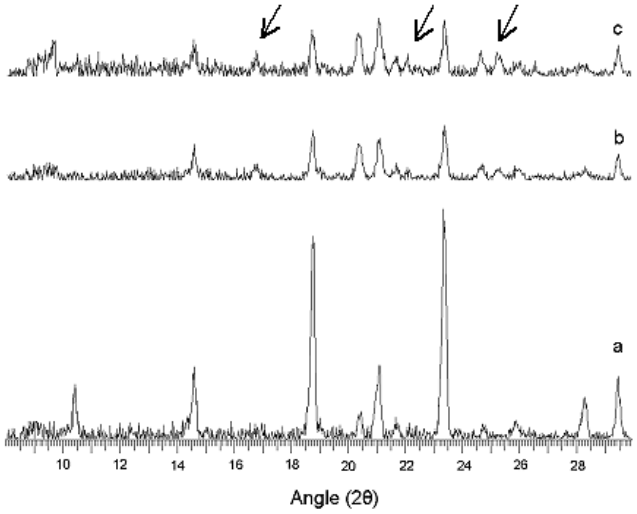

Figure 1. XRPD scans of pure mannitol and mannitol vacuum dried from water and buffer: (a) pure mannitol, (b) mannitol dried from water, (c) mannitol dried from buffer. The arrows represent the peaks that are not present in the XRPD scan of pure mannitol.

Figure 2 shows the XRPD scans of samples vacuum dried from solutions containing different wt/wt ratios of βLg:mannitol and of pure mannitol. No peaks were observed in the XRPD patterns of vacuum-dried samples containing up to 1:5 wt/wt βLg:mannitol, indicating a lack of crystallinity in these samples. This finding indicated that proteins such as βLg have a tendency to inhibit crystallization of mannitol up to a certain wt/wt βLg:mannitol ratio. As the mannitol content was increased up to a 1:15 wt/wt βLg:mannitol ratio in the dried samples, several low intensity peaks were observed in the XRPD scans. From the positions of these low intensity peaks, it seemed that mannitol

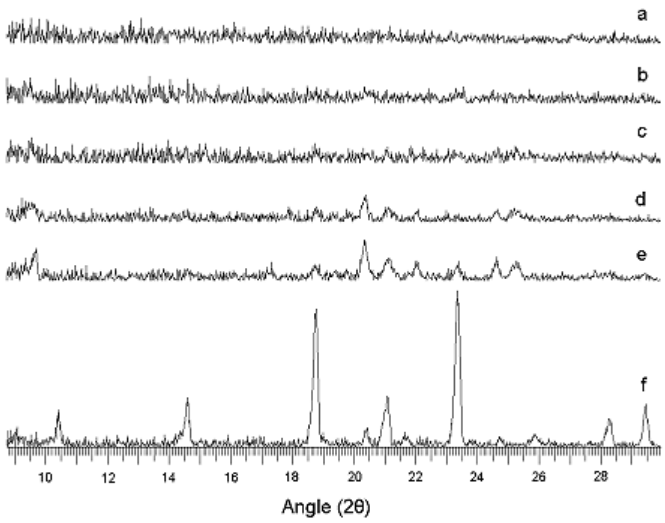

Figure 2. XRPD scans of samples vacuum dried from solutions containing different wt/wt ratios of βLg:mannitol, respectively: (a) 1:1, (b) 1:2, (c) 1:5, (d) 1:10, (e) 1:15, and (f) pure mannitol.

crystallized out as a mixture of polymorphs at higher protein:mannitol ratios. Specifically, peaks at 9.7° and 22° 2θ for the 1:15 wt/wt βLg:mannitol containing dried sample indicated that mannitol crystallized out mainly as a δ-polymorph. The small peak present at 18.7° 2θ and 23.4° 2θ indicated that a small amount of mannitol could be crystallizing out as either α- or β-polymorph.

PLM Studies

Figure 3 shows the PLM images of vacuum-dried samples prepared from solutions containing various ratios of βLg and mannitol as compared with a 1:1 wt/wt physical mixture of βLg:mannitol. The crystalline mannitol appeared as bright white needles as shown in Figure 3A, whereas the protein appeared as black particles in the background because of its amorphous character. When vacuum dried, no evidence of any crystalline mannitol was observed in the 1:1 wt/wt βLg:mannitol containing sample as shown in Figure 3B. This finding supports the results observed in XRPD, which show that protein significantly inhibits mannitol crystallization upon vacuum drying at low protein:mannitol ratios. However, in all of the other samples (Figures 3C-3F), some amount of crystalline mannitol was observed, which was attributed to the brightness in the PLM images of these samples; however, the brightness was far less compared with that observed in the physical mixture. This finding indicated that mannitol was present in these samples both in the amorphous and crystalline forms.

The presence of crystalline mannitol in samples containing as low as 1:2 wt/wt βLg:mannitol, as seen in the PLM images, was an important observation, since no evidence of crystalline mannitol was seen in these samples from XRPD studies. This finding could be due to the low sensitivity of the XRPD to the presence of a slight amount of crystalline material in mixed crystalline/amorphous systems. Based on these results, it can be concluded that PLM is a far more sensitive technique to indicate the presence of crystalline material as compared with XRPD. Although PLM seemed to be a better indicator of the presence of crystalline material in a mixed system, this technique could not be used for the quantification of the crystallinity in the present system primarily because the random distribution of the crystals in the system makes any reproducible quantification difficult. FTIR studies were conducted to further investigate and confirm whether crystalline mannitol was present in lower (less than 1:5 wt/wt) βLg:mannitol-containing dried samples.

FTIR Studies

It has been shown that the FTIR spectra of the 3 polymorphs of crystalline mannitol differ considerably and reflect the difference in the interaction forces between molecules that result from different conformation arrangements in each crystal polymorph.[27] By similar argument, considerable changes in the FTIR spectra should also be observed between the amorphous form and the different crystalline forms of the same material. In general, the peaks observed in a typical FTIR spectrum can be categorized in 2 sections: (1) the "functional group" region from 4000 to 1500 cm^{-1}, in which the peaks are characteristic of specific kinds of bonds and their vibrational modes, and (2) the "fingerprint" region from 1500 to 400 cm^{-1}, where the peaks arise from complex deformations of the whole molecule. The peaks in the fingerprint region are a characteristic of molecular symmetry or combination bands arising from multiple bonds deforming simultaneously and hence are unique to each molecule.

In the present FTIR studies, the whole region of 4000 to 400 cm^{-1} was evaluated in order to gain an understanding of the physical state of mannitol in various dried samples. Figure 4A shows the FTIR spectra of pure mannitol, pure βLg (vacuum-dried βLg in the absence of mannitol), and a 1:1 wt/wt physical mixture of βLg:mannitol in the functional group region. As observed, pure mannitol showed sharp peaks between 3400 cm^{-1} and 3200 cm^{-1} that are characteristic of the O-H stretching vibrations with intermolecular H-bonds. Another set of sharp peaks was observed between 3000 and 2800 cm^{-1}, characteristic of the C-H stretching vibrations. The positions and the number of peaks in these regions related to the β-polymorph of mannitol (compared with spectra described by Yu et al[26]), which was also confirmed earlier by XRPD studies. The FTIR spectrum of pure

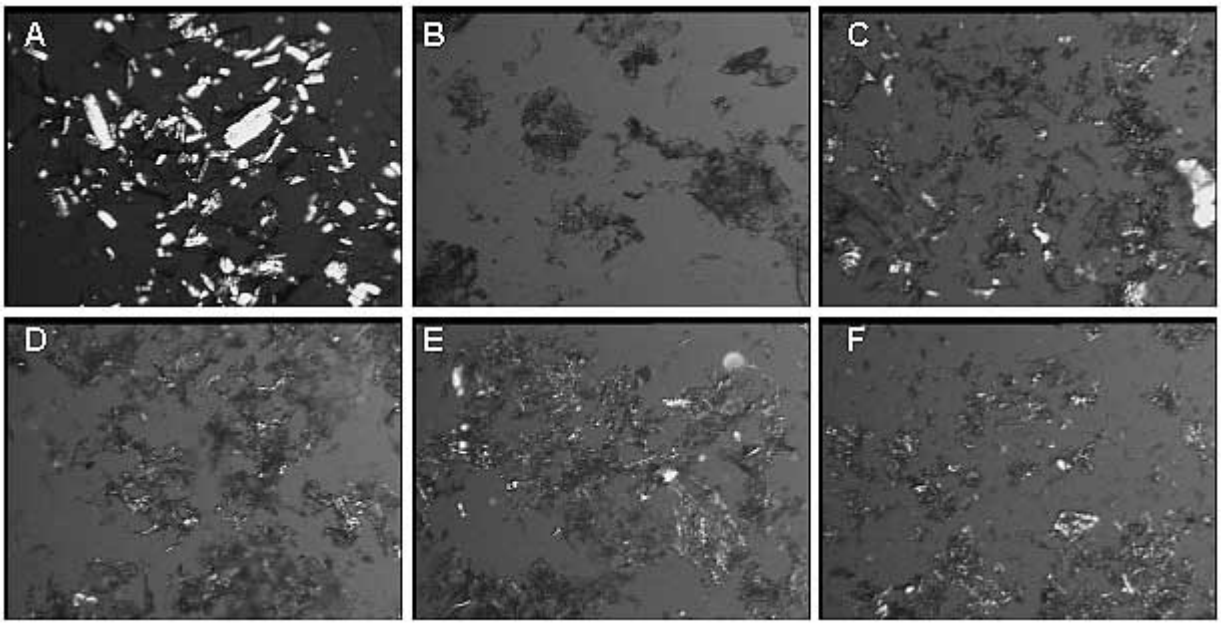

Figure 3. Polarized light microscopy images of samples vacuum dried from solutions containing various wt/wt ratios of βLg:mannitol, respectively: (A) physical mixture of 1:1 wt/wt βLg:mannitol, (B) 1:1, (C) 1:2, (D) 1:5, (E) 1:10, and (F) 1:15. The bright white parts of the images indicate crystallinity in the samples.

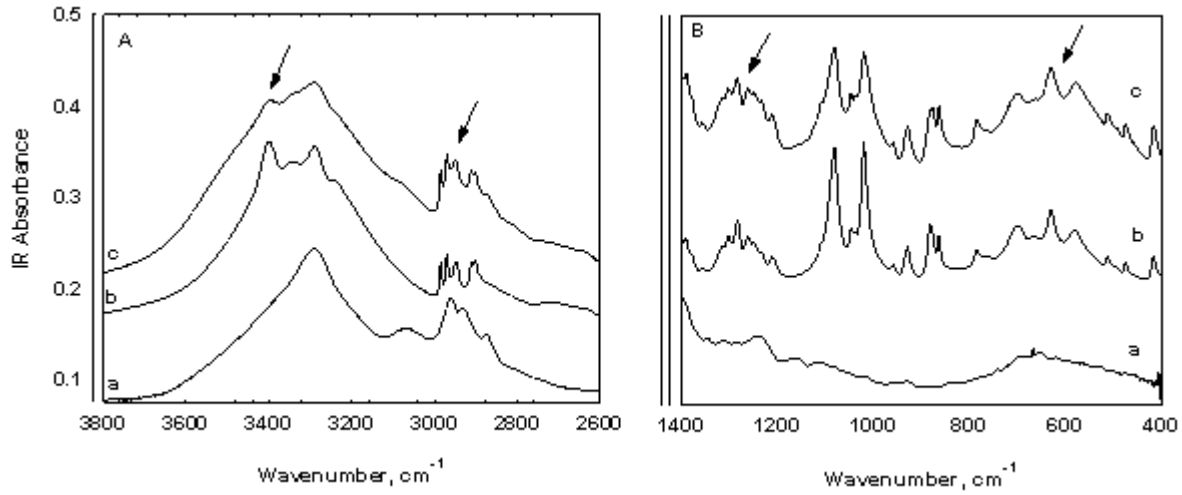

Figure 4. FTIR spectra of (a) pure βLg, (b) pure mannitol and (c) physical mixture of 1:1 wt/wt βLg:mannitol. (A) Functional group region. (B) Fingerprint region. The arrows represent the peaks of interest.

protein in the functional group region showed a broad peak at 3200 cm^{-1} and another set of small peaks in the 3000 to 2800 cm^{-1} region. Since there are several functional groups present in the protein, specific assignment to these peak positions was not attempted. It is sufficient for our purpose that the peak positions and number of peaks differ for pure mannitol and pure protein. Hence, when a physical mixture of βLg and mannitol was prepared in a 1:1 wt/wt ratio, the resulting FTIR spectrum showed peaks that would typically result from the sum of the spectra of the pure compounds. Of special interest in the FTIR spectrum of physical mixture were the peaks at 3380 cm^{-1} and the group of peaks between 3000 and 2800 cm^{-1}.

The fingerprint region (1400-400 cm^{-1}) actually provided a better indicator of the physical state of mannitol since the

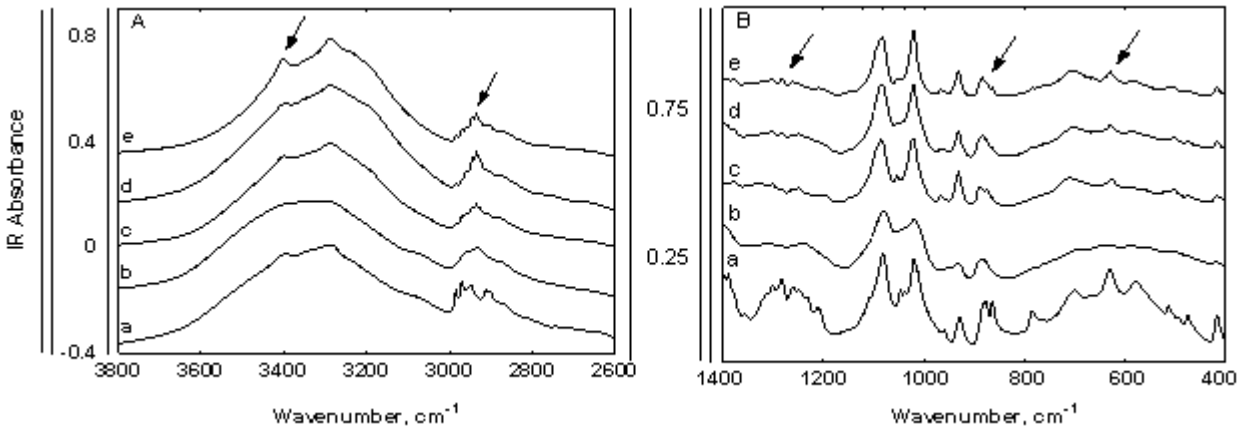

Figure 5. FTIR spectra of samples vacuum dried from solutions containing various wt/wt ratios of βLg:mannitol: (a) physical mixture of 1:1 wt/wt βLg:mannitol, (b) 1:1, (c) 1:2, (d) 1:5, and (e) 1:10. (A) Functional group region. (B) Fingerprint region. The arrows represent the peaks where the changes are most prominent.

protein, βLg, did not exhibit any significant peaks in this region (as shown in Figure 4B). Mannitol, on the other hand, displayed several characteristic peaks in this region. The shape and position of these peaks corresponded to the β-polymorph of mannitol. Because of the pronounced peaks of mannitol in this region as compared with βLg, the shape of the FTIR spectrum of the 1:1 physical mixture of βLg:mannitol mainly resembled the spectrum shape of pure mannitol. This finding was useful as any change in the spectrum shape could be related directly to a change in the physical state of the mannitol.

Figures 5A and 5B show the FTIR scans of vacuum-dried mannitol-βLg samples in various wt/wt ratios and are compared with the FTIR scan of 1:1 wt/wt physical mixture of mannitol and βLg. The FTIR scan of sample containing dried mannitol and βLg present in a 1:1 wt/wt ratio indicated that mannitol loses its crystallinity to a significant extent. This finding was based on the broadening of the peak at 3400 to 3300 cm^{-1}, which was unlike the peaks in the spectra of pure protein or mannitol or the physical mixture in this region. This broadening is attributed to the enormous intermolecular hydrogen bonding in the system as a result of mannitol being present in amorphous state with the protein. The presence of amorphous mannitol was further confirmed by the loss of sharp peaks in the 3000 to 2800 cm^{-1} region and the absence of several peaks in the fingerprint region that were originally present in the physical mixture. The overall absence of sharp peaks in the fingerprint region, resulting in broadening of the spectrum, is a direct indication of mannitol being present in the amorphous form, since none of the crystal forms of mannitol exhibit this behavior. The loss of peaks occurs because of a loss in the specific vibrational modes of the mannitol molecule, which are restricted in a crystal, to the much more widely distributed vibrational modes that are typical of an amorphous system.

As the mannitol proportion was increased in the dried samples compared with βLg, appearance of some of the IR peaks was observed, which were also present in pure crystalline mannitol and in the physical mixture, for example, at 3400 cm^{-1}, in the region of 3000 to 2800 cm^{-1}, and in the fingerprint region. This finding indicated that upon increasing the mannitol proportion in the dried samples from 1:2 to 1:10 wt/wt βLg:mannitol ratios, the crystals of mannitol appeared in the system. However, the intensity of these peaks was not as high as seen in the 1:1 physical mixture of mannitol and βLg, which indicated that there was amorphous mannitol present in the system as well. The intensity of these peaks increased proportionally to the mannitol amount in the system, further indicating that the crystallization of mannitol depended strongly on the βLg to mannitol ratio. It is important to mention again that the presence of crystalline mannitol was not evident in low mannitol-containing dried samples from XRPD studies such as in 1:2 or 1:5 wt/wt βLg:mannitol samples. These samples, however, did show the presence of a slight amount of crystalline mannitol as indicated by the reappearance of certain low-intensity peaks characteristic of crystalline mannitol in FTIR studies as was also indicated by the PLM studies. Hence, FTIR spectroscopy appeared to be more sensitive than XRPD in picking up small quantities of crystalline material in a largely amorphous system.

Modulated Differential Calorimetry Studies

MDSC studies were performed to characterize the amorphous mannitol present in various vacuum-dried βLg-

mannitol systems. MDSC was used in order to clearly study the various events that could be seen in a typical thermogram for an amorphous system such as glass transition, recrystallization, protein denaturation, and mannitol melting. The theory behind MDSC is well documented in literature.[31,32] In brief, for the purpose of present studies, the reversible heat flow characterizes the "reversing" events such as glass transition, whereas the nonreversible heat flow characterizes events such as enthalpy relaxation and crystallization. Hence, MDSC can be used to deconvolute events that may take place in a complex system. Figure 6 represents the reversible heat flow, nonreversible flow, and the total heat flow in a MDSC scan for a vacuum-dried 1:1 wt/wt βLg:mannitol system. Several events are evident in this scan. The presence of amorphous mannitol in the dried sample was confirmed by the presence of glass transition, T_g, which is most evident in the reversible heat flow thermogram and has a midpoint around 33.4°C (shown in the inset). The glass transition was followed by the crystallization of mannitol as shown by the presence of crystallization exotherm in the nonreversible heat flow thermogram (crystallization exotherm will not appear in the reversible heat flow thermogram). The final 2 events represented the protein denaturation endotherm around 130°C (based on DSC of pure vacuum-dried protein) and melting endotherm of the crystalline mannitol around 142°C (lower temperature than that of pure mannitol due to presence of protein as the impurity).

As shown in the inset of Figure 6, the glass transition midpoint of amorphous mannitol appears around 33.4°C, which is significantly higher than the reported glass transition midpoint of the pure amorphous mannitol (13°C-15°C).[20] This finding indicates that at least a part of the amorphous mannitol existed in a single amorphous phase with the amorphous protein, and the resulting glass transition midpoint is the weighted average of the glass transitions of the 2 components. This is important because for both the "vitrification theory" and the "water-substitution theory" of stabilization of proteins in the dried state, the primary criterion for an effective stabilizer is that it must be present in a single amorphous phase with the protein. Hence, mannitol could serve as an effective stabilizer of proteins during drying as long as it remains amorphous in the system.

Figure 7 represents the total heat flow thermograms for dried samples that contained βLg:mannitol in the range of 1:2 to 1:10 wt/wt ratios. The crystallization exotherm is clearly seen in all thermograms, indicating the presence of amorphous mannitol in all of the initial samples. Furthermore, the crystallization exotherms appeared at lower temperatures for increasing amounts of mannitol in dried samples, indicating enhanced susceptibility of the amorphous mannitol to crystallize as the mannitol proportion

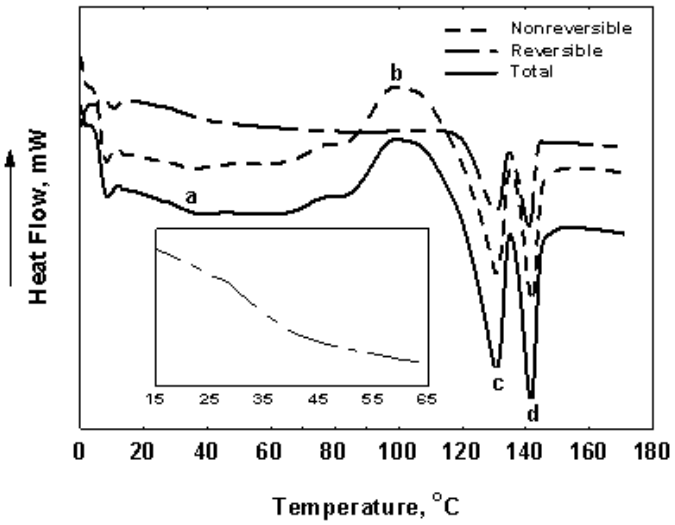

Figure 6. MDSC thermogram of vacuum-dried 1:1 wt/wt βLg:mannitol showing the reversible, nonreversible, and total heat flow. Various events indicated are (a) mannitol glass transition (expanded in the inset), (b) mannitol recrystallization, (c) protein denaturation, and (d) mannitol melting.

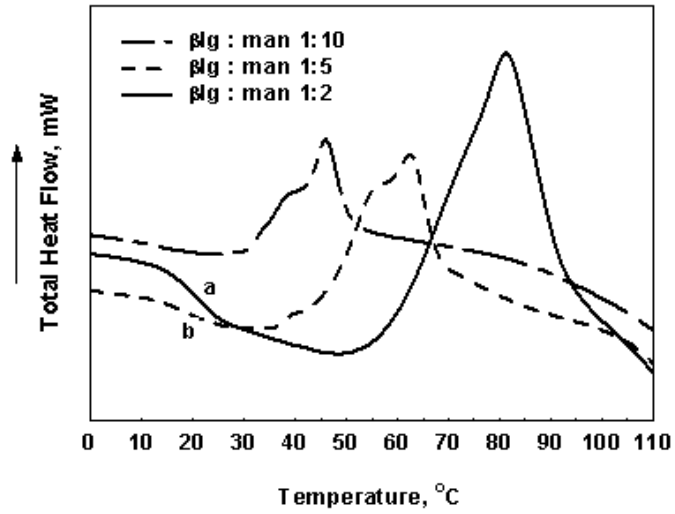

Figure 7. Total heat flow in MDSC thermograms indicating crystallization exotherms of mannitol in samples vacuum dried from solutions containing various wt/wt ratios of βLg:mannitol. (a) T_g midpoint at 20°C. (b) T_g midpoint at 17.5°C.

is increased. Of interest, the areas under the crystallization exotherms decreased with increasing mannitol proportion in the dried sample. Considering that these thermograms were normalized for the weight of mannitol, this observation indicated that the ratio of the amorphous to crystalline mannitol decreased with an increase in the overall amount of mannitol in the dried protein-mannitol samples. Hence, it can be concluded that as the mannitol ratio is increased in the vac-

Table 2. Normalized Heats of Crystallization for the Amorphous Mannitol in Various wt/wt Ratios of βLg:Mannitol-Dried Samples From The MDSC Scans and Results of the Calculations Indicating Ratio of βLg:Amorphous Mannitol in the Dried Samples*

βLg:Mannitol Ratio, wt/wt	Sample Weight in DSC Pan, mg†	Mannitol amount, mg†	Normalized Heat of Crystallization, J/g‡	% Amorphous Mannitol	Amorphous Mannitol Content, mg	Protein: Amorphous Mannitol Ratio, wt/wt
1:1	9.5	4.25	128.5 ± 11.1	100%	4.25	1:1
1:2	7.3	4.82	64.3 ± 4.2	50.07%	2.41	1:0.97
1:5	7.3	6.08	24.64 ± 2.1	19.17%	1.217	1:0.95
1:10	6.1	5.54	10.59 ± 0.9	8.24%	0.555	1:0.85

*MDSC indicates modulated differential scanning calorimetry.
†Only single values are presented to represent the amount of mannitol in each wt/wt ratio.
‡Values are mean (n = 3) ± SD.

uum-dried mannitol-βLg samples, mannitol is present in both crystalline and amorphous forms with the crystalline mannitol amount increasing with an increase in total mannitol proportion. This finding could be an indication of the fact that there is only a fixed ratio of βLg:mannitol that keeps the mannitol amorphous and the rest of the mannitol crystallizes out.

To further confirm that this is indeed the case, attempt was made to quantify amorphous mannitol in the dried samples by calculating areas under the crystallization exotherm for samples containing different βLg:mannitol wt/wt ratios. The assumption was that whatever amorphous mannitol was present in the initial dried sample crystallized out and exhibited a crystallization exotherm in the MDSC scan. The advantage offered by this method was that even if mannitol crystallized out as different polymorphs, the total area under the crystallization exotherm would still represent crystallization from total amorphous mannitol in the initial dried samples. The sample containing βLg:mannitol in a 1:1 wt/wt ratio was considered to be completely amorphous as also indicated by XRPD, PLM, and FTIR studies. Hence, the normalized heat of crystallization per gram of mannitol for this sample would arise from all of the mannitol present. In a similar way, normalized heat of crystallization was also obtained for other samples containing different wt/wt ratios of βLg:mannitol. The results are shown in Table 2. As shown in the table, the normalized heats for higher βLg:mannitol ratios decreased with an increase in the mannitol proportion in the sample. If all of the mannitol was amorphous in all samples, then after normalization for the mannitol weight, similar heat of crystallization data should have been obtained. This is clearly not the case. This finding indicates that samples with 1:2 or higher wt/wt βLg:mannitol ratios contained both amorphous and crystalline mannitol as was also observed through other techniques.

To calculate the amount of amorphous mannitol and the exact ratio of protein to amorphous mannitol in the dried samples, percentage of amorphous mannitol was obtained by dividing the heat of crystallization obtained for 1:2 wt/wt and higher βLg:mannitol-containing samples by the heat of crystallization of the 1:1 wt/wt βLg:mannitol sample. From this percentage, the amount of amorphous mannitol was obtained in each sample. The amount of amorphous mannitol was then divided by the amount of protein, to obtain the protein to amorphous mannitol ratio. These results are shown in Table 2. It can be seen that with increasing βLg:mannitol ratio in the dried samples, the protein:amorphous mannitol wt/wt ratio does not increase above 1:1 and decreases only slightly with an increase in the initial βLg:mannitol wt/wt ratios. This was an important observation and indicated the presence of specific interactions between βLg and mannitol. These results were consistent with PLM and FTIR studies, which showed the absence of crystalline mannitol at 1:1 wt/wt ratio, whereas crystalline mannitol was clearly observed in 1:2 and higher wt/wt ratios.

If the wt/wt ratio of protein:amorphous mannitol does not change significantly with the change in the initial protein:mannitol wt/wt ratio, then the T_g of the system should remain constant, independent of the initial protein:mannitol ratios. However, a decrease in the T_g was observed upon increase in the protein:mannitol ratio (see Figure 7) indicating that a higher amount of amorphous mannitol may be present in the dried state as compared with that calculated from the crystallization exotherms. This is also indicated by the XRPD studies, where no characteristic peaks of mannitol were observed, even though the results of the calculations indicated presence of more than 50% crystalline mannitol. A plausible explanation for this inconsistency is that the crystallization of mannitol is affected in the temperature scanning mode. In other words, crystallization of mannitol occurs as a function of increasing temperature with time in

DSC, which could result in a lower estimate of amorphous mannitol as compared with crystallization at constant temperature. Hence, the estimate of the amorphous mannitol from the crystallization exotherm in DSC studies should be accepted with a little caution.

Overall, from the above studies it can be concluded that proteins have a general tendency to inhibit the crystallization of mannitol and thus retain mannitol in the amorphous state. FTIR and PLM seemed to be better indicators of presence of small amounts of crystallinity in the mixed amorphous/crystalline systems. At least part of amorphous mannitol was present in the single phase with the protein, and the MDSC studies indicated that the wt/wt ratio of the protein:amorphous mannitol is relatively fixed and is independent of the initial protein:mannitol wt/wt ratio in the dried samples. The next step was to study the effect of the physical state of mannitol on the secondary structure of protein by use of FTIR spectroscopy.

Secondary Structure of Proteins in Vacuum-Dried Samples Containing Mannitol: Second Derivative FTIR Studies

FTIR studies were performed in order to investigate the effect of the physical state of mannitol and the amount of mannitol in the dried samples on the secondary structure of 2 proteins, βLg and rhIFN, after vacuum drying. The 2 proteins differ significantly with regard to their secondary structure (βLg predominantly has beta sheets, whereas IFNα2a is an all alphα-helical protein). Hence, the purpose of these studies was to study the effect of initial protein:mannitol wt/wt ratio on the structure of 2 different proteins in the dried state following vacuum drying. This was done by qualitatively comparing the area-normalized second derivative FTIR spectra of proteins in the amide I (1700-1600 cm^{-1}) region. Mannitol did not show any IR band in this region (data not shown).

Figure 8 shows the area-normalized second-derivative spectra of βLg vacuum dried in the presence of varying amounts of mannitol as compared with the vacuum dried βLg (in the absence of mannitol) and βLg in solution at pH 7.4. The second derivative FTIR spectrum of βLg solution shows several peaks that can be assigned to various secondary structure components in this protein. The most intense band is observed at 1631 cm^{-1}, which is indicative of the extensive β-sheet structure in this protein.[33] The band at 1661 cm^{-1} can be attributed to the β-turns or to the α-helices present in βLg. The other bands observed at 1684 cm^{-1} and at 1693 cm^{-1} indicated the antiparallel β-sheet content in βLg.[33,34] As compared with the second derivative FTIR of βLg in solution, vacuum-dried βLg shows a significant loss in the intensity of the band at 1631 cm^{-1}. It is generally accepted that a decrease in the intensity of the band in a second-derivative FTIR spectra relates to a decrease in the content of the associated secondary structure. The shift in the position of the peak represents a change in the hydrogen bonding pattern, and hence, also relates to changes in the secondary structure of the protein. Alternatively, the shift may be simply due to the dehydration of the sample. However, from the intensity differences, it can be concluded that the vacuum-dried βLg shows a significant decrease in the β-sheet structure compared with βLg solution structure.

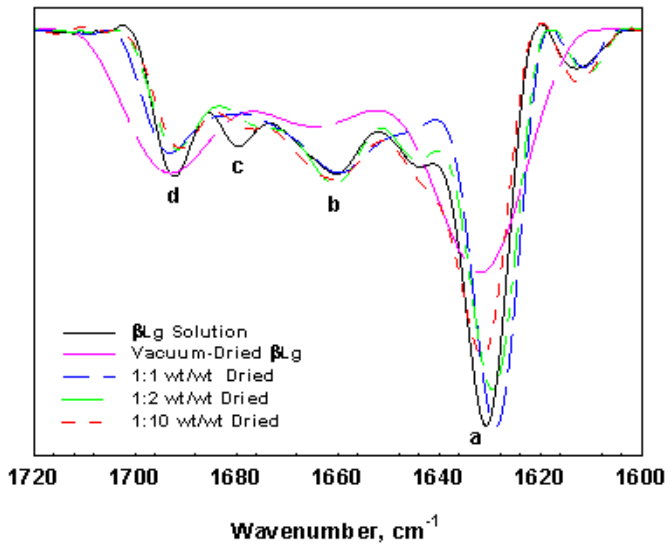

Figure 8. Area-normalized second derivative FTIR spectra of βLg vacuum dried from solutions containing various wt/wt ratios of βLg:mannitol as compared with βLg in solution and vacuum-dried βLg. (a) 1631 cm^{-1}, (b) 1661 cm^{-1}, (c) 1683 cm^{-1}, and (d) 1693 cm^{-1}.

When vacuum dried in the presence of mannitol, significant changes in the FTIR spectra of βLg were observed in the intensity of different bands. When dried from a 1:1 wt/wt βLg:mannitol solution, no significant change in the intensity of the band at 1631 cm^{-1} was observed, although, a slight shift in the peak minimum was observed. The slight shift as well as changes in the side bands indicated slight changes in the secondary structure of βLg. With further increase in the mannitol content to 1:10 wt/wt βLg:mannitol ratio, the intensity of band at 1631 cm^{-1} decreased significantly, and this decrease was proportional to the increase in the total mannitol amount in the dried sample. This decrease indicated a loss in the β-sheet content of the protein; however, the loss was not to an extent as seen in the lyophilized sample. These results suggested that the amount of mannitol in the system has significant effect on the secondary structure of the protein, βLg. The most native-like structure is observed in the 1:1 wt/wt βLg:mannitol-containing vacuum-dried sample, which is relatively lost upon further increasing mannitol

proportion. Since it was shown by MDSC studies that the protein:amorphous mannitol remained relatively fixed, it seems that the presence of crystalline mannitol somehow affects the βLg secondary structure.

There are a few reports in literature in which similar observations have been made indicating that the presence of crystalline mannitol could affect the secondary structure and stability of proteins.[22,23] The exact mechanism is not known; however, it can be speculated that the crystallization could affect the distribution of the amorphous mannitol around the protein molecules and hence affect the protein secondary structure. No attempt is made in the present studies to elucidate the exact mechanism of this behavior. Future studies will be performed based on controlled crystallization of mannitol within the same sample to understand this behavior in greater detail.

Figure 9 shows the area-normalized second derivative FTIR spectra of vacuum-dried IFNα2a in the presence of varying amounts of mannitol as compared with IFNα2a solution at pH 5.0. In the absence of mannitol, IFNα2a solution shows a major band at 1654 cm^{-1} that is characteristic of the presence of a-helices in this protein.[32] When dried from solutions containing different wt/wt ratios of IFNα2a:mannitol, a rather random pattern was observed in terms of the change in intensity at 1654 cm^{-1} with an increase in mannitol content unlike that observed for βLg, where the intensity decreased monotonically with an increase in mannitol content. The most significant loss in intensity was observed in 1:1 wt/wt IFNα2a:mannitol-containing sample, whereas the intensities of the peak at 1654 cm^{-1} for 1:2 and 1:5 wt/wt IFNα2a:mannitol-containing samples were more or less close to that of the FTIR spectrum of IFNα2a in solution. A slight shift in the peak minimum, however, was observed in all dried samples as compared with the solution IFNα2a.

These results suggest that for an α-helical protein such as IFNα2a, the increase in mannitol proportion in fact increases the α-helical content thus making IFNα2a more native-like in solid state. Whereas, for a protein that is rich in β-sheets such as βLg, the β-sheet content decreases with an increase in total mannitol content. However, these conclusions cannot be generalized to all proteins and are specific to the 2 proteins used in this study only. More studies on a variety of other proteins will help in understanding the general nature of the effect of mannitol physical state on protein secondary structure in the dried state.

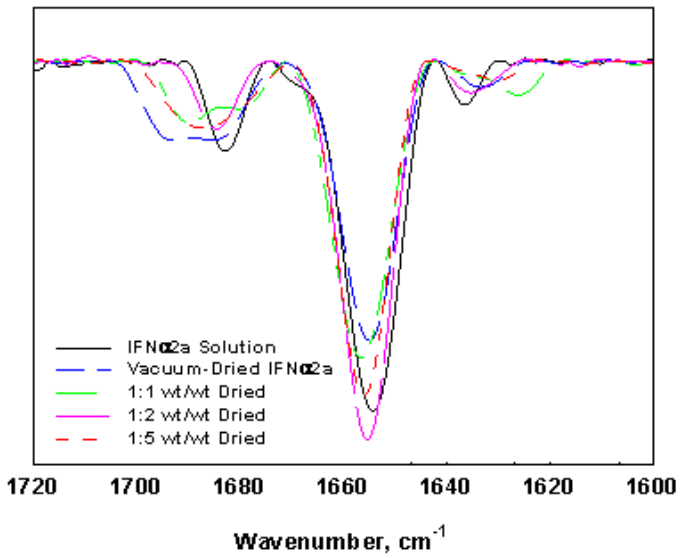

Figure 9. Area-normalized second derivative FTIR spectra of IFNα2a vacuum dried from solutions containing various wt/wt ratios of IFNα2a:mannitol compared with IFNα2a solution and vacuum-dried IFNα2a.

CONCLUSION

It is concluded from the present studies that the estimation of the amorphous mannitol content in a mixed amorphous/crystalline system is affected by the technique used. PLM is far more sensitive to the presence of crystalline material than XRPD. The protein secondary structure is affected by the amount of crystalline mannitol in the system and these structural changes are protein specific.

ACKNOWLEDGEMENTS

The authors gratefully acknowledge financial support from the National Science Foundation Industry/University Cooperative Research Center for Pharmaceutical Processing (http://www.ipph.purdue.edu/~nsf/aboutCPPR.html) and Hoffmann-La Roche, Nutley, NJ, for the donation of interferon α-2a samples. The authors also acknowledge Dr M.J. Pikal for his helpful suggestions.

REFERENCES

1. Pikal MJ. Freeze-drying of proteins: Process, formulation, and stability. In: Cleland JL, Langer R, eds. *Formulation and Delivery of Proteins and Peptides*. Washington DC: American Chemical Society; 1994:120-133.

2. Wang W. Lyophilization and development of protein pharmaceuticals. *Int J Pharm*. 2000;203:1-60.

3. Mumenthaler M, Hsu CC, Pearlman R. Feasibility study on spray-drying protein pharmaceuticals: Recombinant human growth hormone and tissue-type plasminogen activator. *Pharm Res*. 1994;11:12-20.

4. Maa YF, Nguyen PA, Andya JD, et al. Effect of spray drying and subsequent processing conditions on residual moisture content and physical/biochemical stability of protein inhalation powders. *Pharm Res*. 1998;15:768-775.

5. Mumenthaler M, Leuenberger H. Atmospheric spray-freeze-drying: A suitable alternative in freeze-drying technology. *Int J Pharm*. 1991;72:97-110.

6. Shenoy B, Wang Y, Shan W, Margolin AL. Stability of crystalline proteins. *Biotechnol Bioeng*. 2001;73:358-369.

7. Winters MA, Knutson BL, Debenedetti PG, et al. Precipitation of proteins in supercritical carbon dioxide. *J Pharm Sci*. 1996;85:586-594.

8. Moshashaee S, Bisrat M, Forbes RT, Nyqvist H, York P. Supercritical fluid processing of proteins. I: Lysozyme precipitation from organic solution. *Eur J Pharm Sci*. 2000;11:239-245.

9. Mattern M, Winter G, Rudolph R, Lee G. Formulation of proteins in vacuum-dried glasses. I: Improved vacuum-drying of sugars using crystallizing amino acids. *Eur J Pharm Biopharm*. 1997;44:177-185.

10. Brohnstein V. Scalable long-term shelf preservation of sensitive biological solutions and suspensions. US patent 6 509 146, January 21, 2003.

11. Manning MC, Patel K, Borchardt RT. Stability of protein pharmaceuticals. *Pharm Res*. 1989;6:903-918.

12. Arakawa T, Prestrelski S, Kenney WC, Carpenter JF. Factors affecting short-term and long-term stabilities of proteins. *Adv Drug Deliv Rev*. 2001;46:307-326.

13. Wang W. Instability, stabilization, and formulation of liquid protein pharmaceuticals. *Int J Pharm*. 1999;185:129-188.

14. Prestrelski SJ, Tedischi N, Arakawa T, Carpenter JF. Dehydration-induced conformational transitions in proteins and their inhibition by stabilizers. *Biophys J*. 1993;65:661-671.

15. Carpenter JF, Crowe JH. An infrared spectroscopic study of the interaction of carbohydrates with dried proteins. *Biochemistry*. 1989;28:3916-3922.

16. Allison SD, Chang B, Randolph TW, Carpenter JF. Hydrogen bonding between sugar and protein is responsible for inhibition of dehydration-induced protein unfolding. *Arch Biochem Biophys*. 1999;365:289-298.

17. Duddu SP, Dal Monte PR. Effect of glass transition temperature on the stability of lyophilized formulations containing a chimeric therapeutic antibody. *Pharm Res*. 1997;14:591-595.

18. Franks F, Hatley RHM, Mathias SF. Materials science and the production of shelf-stable biologicals. *BioPharm*. 1991;4:38-42,55.

19. Liu R, Langer R, Klibanov AM. Moisture-induced aggregation of lyophilized proteins in the solid state. *Biotechnol Bioeng*. 1991;37:177-184.

20. Kim AI, Akers MJ, Nail SL. The physical state of mannitol after freeze-drying: Effects of mannitol concentration, freezing rate, and a non-crystallizing solute. *J Pharm Sci*. 1998;87:931-935.

21. Cavatur RK, Suryanarayanan R. Characterization of phase transitions during freeze-drying by in situ X-ray powder diffractometry. *Pharm Dev Technol*. 1998;3:579-586.

22. Izutsu K, Yoshioka S, Terao T. Effect of mannitol crystallization on the stabilization of enzymes during freeze-drying. *Chem Pharm Bull (Tokyo)*. 1994;42:5-8.

23. Izutsu K, Kohima S. Excipient crystallinity and its protein-structure-stabilizing effect during freeze-drying. *J Pharm Pharmacol*. 2002;54:1033-1039.

24. Costantino HR, Andya JD, Nguyen PA, et al. Effect of mannitol crystallization on the stability and aerosol performance of a spray-dried pharmaceutical protein, recombinant anti-IgE monoclonal antibody. *J Pharm Sci*. 1998;87:1406-1411.

25. Capan Y, Jiang G, Giovagnoli S, Na K-H, DeLuca PP. Preparation and characterization of poly(D,L-lactide-co-glycolide) microspheres for controlled release of human growth hormone. *AAPS PharmSciTech*. 2003;4(2):article 28.

26. Yu L, Milton N, Groleau EG, Mishra DS, Vansickle RE. Existence of a mannitol hydrate during freeze-drying and practical implications. *J Pharm Sci*. 1999;88:196-198.

27. Burger A, Henck JO, Hetz S, Rollinger JM, Weissnicht AA, Stottner H. Energy/temperature diagram and compression behavior of the polymorphs of D-mannitol. *J Pharm Sci*. 2000;89:457-468.

28. Cannon AJ, Trappler EH. The influence of lyophilization on the polymorphic behavior of mannitol. *PDA J Pharm Sci Technol*. 2000;54:13-22.

29. Prestrelski SJ, Tedeschi N, Arakawa T, Carpenter JF. Dehydration-induced conformational transitions in proteins and their inhibition by stabilizers. *Biophys J*. 1993;65:661-671.

30. Prestrelski SJ, Arakawa T, Carpenter JF. Separation of freezing- and drying-induced denaturation of lyophilized proteins using stress-specific stabilization. II. Structural studies using infrared spectroscopy. *Arch Biochem Biophys*. 1993;303:465-473.

31. Jones KJ, Kinshott I, Reading M, Lacey AA, Nikolopoulos C, Pollock HM. The origin and interpretation of the signals of MTDSC. *Thermochim Acta*. 1997;304-305:187-189.

32. Gmelin E. Classical temperature-modulated calorimetry: A review. *Thermochim Acta*. 1997;304-305:1-26.

33. Dong A, Huang P, Caughey WS. Protein secondary structures in water from second-derivative amide I infrared spectra. *Biochemistry*. 1990;29:3303-3308.

34. Bandekar J. Amide modes and protein conformation. *Biochim Biophys Acta*. 1992;1120:123-143.